NASA TECHNICAL MEMORANDUM

NASA TM-73843

NASA TM-73843

SMALL-SIGNAL GAIN DIAGNOSTIC MEASUREMENTS IN A FLOWING CO_2 PIN DISCHARGE LASER

by R. A. Blech, E. J. Manista, and J. W. Dunning, Jr.
wis Research Center
Cleveland, Ohio 44135

November 1977

1. Report No. NASA TM-73843	2. Government Accession No.	3. Recipient's Catalog No.
4. Title and Subtitle SMALL-SIGNAL GAIN DIAGNOSTIC MEASUREMENTS IN A FLOWING CO_2 PIN DISCHARGE LASER		5. Report Date November 1977 6. Performing Organization Code
7. Author(s) R. A. Blech, E. J. Manista, and J. W. Dunning, Jr.		8. Performing Organization Report No. E-9430 10. Work Unit No.
9. Performing Organization Name and Address National Aeronautics and Space Administration Lewis Research Center Cleveland, Ohio 44135		11. Contract or Grant No. 13. Type of Report and Period Covered Technical Memorandum
12. Sponsoring Agency Name and Address National Aeronautics and Space Administration Washington, D.C. 20546		14. Sponsoring Agency Code
15. Supplementary Notes		

16. Abstract

Small-signal gain diagnostic measurements were conducted on the NASA-Lewis Research Center's closed loop, high power, carbon dioxide laser to assess the coupling between gas flow velocity and resonator saturation. Parameters investigated included optical cavity and multi-pin to plane excitation configurations as well as laser gas flow velocity and discharge power. Results of gain measurements within and downstream of the excitation volume are presented for a laser gas composition ($He:N_2:CO_2$) of 10:7:1 at 90 torr. The gain at constant discharge power was observed to be dependent upon discharge power level and time. An important result of this study is that the effects of gain swept downstream of the discharge region must be considered in the resonator design if efficient extraction of stored optical energy is desired.

17. Key Words (Suggested by Author(s)) CO_2 High powered lasers Laser plasma diagnostics	18. Distribution Statement Unclassified - unlimited STAR Category 36		
19. Security Classif. (of this report) Unclassified	20. Security Classif. (of this page) Unclassified	21. No. of Pages	22. Price*

* For sale by the National Technical Information Service, Springfield, Virginia 22161

SMALL-SIGNAL GAIN DIAGNOSTIC MEASUREMENTS IN A FLOWING CO_2 PIN DISCHARGE LASER

by R. A. Blech, E. J. Manista, and J. W. Dunning, Jr.

Lewis Research Center

E-9430

INTRODUCTION

Measurements of the spatial distribution of small signal gain have been reported (refs. 1 and 6) which indicate that the peak gain in a nonlasing, flow-stabilized, transverse pin discharge occurs downstream of the last row of pins. It has been suggested in reference 1 that this observation is qualitatively consistent with a displacement of the discharge current distribution arising from a coupling of the ion drift velocity and the gas flow velocity. The flow velocity dependence of the gain displacement was not, however, reported. Further, reference 1 observed that the peak gain decays exponentially with increasing downstream distance due to the relaxation of the nitrogen excited state. The results of the above studies indicate that efficient extraction of laser energy from a transversely excited, flow-stabilized laser is influenced by both resonator-discharge configuration and laser gas flow velocity. As part of the overall parameterization program involving the Lewis High Power Laser device, a study of the small signal gain present downstream of both the optics and the active excitation volume was undertaken to gain a better understanding of the displaced gain-flow velocity phenomenon. Parameters investigated include optical cavity and excitation configurations, gas flow velocity, and discharge power.

EXPERIMENTAL CONFIGURATION

The test section of the NASA-Lewis High Power CO_2 Laser is shown pictorially in figure 1. It is approximately 1.4 meter in the flow direction by 1.5 meter in the optics direction. The flow-stabilized, self-sustained discharge is generated between the tungsten cathode pins and the copper anode plate spaced 5 centimeters apart for this study. Currents of up to 30 milliamps per pin are possible with flow velocities ranging from 50 to 150 meters per second. The flow direction, optic axis and discharge direction are mutually orthogonal. Five channels are available for excitation and optics, with only one excitation channel used for this study. Up to 21 rows of pins per channel may be connected, with each row alternately consisting of 66 or 64 pins. The pins are spaced such as to provide a pin density of 1 pin per square centimeter. One of the optical configurations used was a single pass unstable resonator with a magnification of 1.26. A multipass optical configuration with single channel excitation was also investigated. Detailed specifications for the test section and Lewis laser in general can be found in reference 2.

A schematic of the small signal gain experimental setup is shown in figure 2. A line selectable, 3-watt water-cooled CO_2 laser is chopped at a frequency of 100 hertz and is divided into a probe beam and reference beam by a 40/60 germanium beam splitter. The transmitted beam enters and leaves the test cavity at the midplane between the electrodes through potassium chloride windows and is detected by pyroelectric detector A.

The reflected beam is further divided by a sodium chloride beam splitter. The transmitted part of this beam is monitored by a spectrum analyzer to assure operation on the P(20) CO_2 laser line. The reflected beam is measured by pyroelectric detector B and provides a reference signal. The signals are conditioned by lock-in amplifiers, and the ratio of the probe beam

signal to the reference beam signal is displayed by a ratiometer. This ratio technique provides a measurement of the small signal gain coefficient which is insensitive to intensity variations in the source laser.

The small signal gain coefficient g_o can be determined using the following equation (ref. 3).

$$I_A = KI_o e^{g_o L} \tag{1}$$

where I_A is the amplified beam intensity, I_o is the initial intensity, K is an instrument constant, and L is the active path length, in this case 135 centimeters. Equation (1) applies when $I_A < I_{sat}$, where I_{sat} is the saturation intensity of the medium. Normalizing equation (1) to a reference intensity I_B results in:

$$g_o = \left[\ln\left(\frac{I_A}{I_B}\right) - \ln\left(\frac{I_A}{I_B}\right)_o\right]\frac{100}{L} \quad \text{percent-cm}^{-1} \tag{2}$$

where I_A/I_B is the measured quantity. For each set of data, the baseline reading $(I_A/I_B)_o$ was taken without a discharge present at the operating conditions of pressure and flow velocity. Absorption of the probe beam by the unexcited medium was negligible at the gas pressures used in this study. Variations of at most a few percent were observed in $(I_A/I_B)_o$ from the beginning to the end of each data run.

RESULTS

Experimental results have been obtained which characterize the behavior of the small-signal gain coefficient as a function of the discharge and flow parameters of the NASA High Power CO_2 laser. The laser gas mixture used for this study was a 10:7:1 $He:N_2:CO_2$ combination at a pressure of 90 torr. Figure 3 shows

the discharge geometry for the measurements made. The first set of data were taken at observation point "A" which was located under row 15, 7.8 centimeters downstream of row 1. This point of observation was chosen since it was well within the volume of the excited medium and yet not obscured by the walls of the test section. No mirrors were used, i.e., no laser beam was extracted, and 21 rows of pins were active. A summary of the discharge power and mass flow variations imposed on three gas loads is given in table I. The results of the gain measurements are plotted in figure 4(a) as a function of gas flow velocity with average discharge power as a parameter. For a fixed average discharge power, the gain coefficient within the excitation volume was observed to decrease linearly with increasing gas flow velocity. The measured gain at constant discharge power also exhibited a dependence upon discharge power level and time. In figure 4(a), for the 55 and 77 kilowatt runs, the straight lines are drawn through the data points measured within 15 minutes and 9 minutes of the establishment of the discharge, respectively; that is, before gas compositional changes produced by the discharge occurred. For the nominal 31 kilowatt case, the straight line has been drawn through the data points measured during the latter part of that run; that is, for discharge times greater than 14 minutes.

These gas compositional effects are more evident in figure 4(b), wherein the gain is plotted against specific discharge power for the aforementioned test conditions. Specific discharge power is defined as input discharge power divided by mass flow rate and is a measure of input energy per unit mass of laser gas. Referring to figure 4(b), the gain data from the three gas loads are observed to fall onto two distinct straight lines. Specifically if we exclude for consideration the gain measured "late" in the two high power runs for 55 and 77 kilowatts, corresponding to discharge times of greater than 15 and 10 minutes, respectively, the measured gain at point A is observed to increase linearly with specific discharge power.

This observation implies that gas heating which leads to an increase in the population density of the lower laser level and consequently eventual saturation of the small-signal gain is negligible for the specific input powers shown. Gas temperatures measured downstream of the discharge volume during these runs indicated maximum temperatures of 356 and 360 K.

Again referring to figure 4(b), the low power 31 kilowatt gain data is observed to fall on a different straight line after excluding the measurements corresponding to discharge times greater than 21 minutes. We suspect the following two reasons are the cause of this behavior. In the two high power runs of 55 and 77 kilowatt, the discharge power level was quickly established and then held constant, whereas in the lower power run the constant level of 31 kilowatt was preceeded by a 12 minute long discharge power variation during which the discharge power was varied from 13 up to 77 kilowatt. Hence sufficient time had elapsed to cause discharge induced gas compositional changes to occur thereby altering the excitation rate of the upper laser level. Another possible explanation for the decreased gain observed at 31 kilowatts is that the spatial distribution of the row currents is different from that obtained in the two high discharge powers; that is, at 31 kilowatts the upstream portion of the discharge is not yet fully developed. Consequently since the excitation rate of the upper laser level is dependent upon current density, variations in the spatial distribution of the discharge current can lead to variations in the small-signal gain coefficient.

The flow velocity dependence of the gain within the discharge would be expected to have a significant bearing on the optical configuration used to produce a laser beam output from the discharge. The first optical and excitation arrangement evaluated was a single pass, 5 centimeter diameter, unstable resonator with the first 16 rows of pins excited. In this configuration the centerline of the 5 cm diameter optics lies along the eleventh row of pins. Thus,

rows 17 through 21 are not excited since they are physically outside of the extraction optics, as shown in figure 3. The small-signal gain was measured at point "B" in the figure, which was located 16 centimeters downstream from the last row of excited pins. Figure 5 shows the laser beam output power and downstream small-signal gain as a function of laser gas flow velocity for the above configuration. The discharge power was held constant for these data points and the laser beam power was determined by absorbing it in a water cooled, NBS calibrated power meter. Figure 5 shows that substantial gain is present downstream of the optics. Much of this gain may be attributed to the long lifetime of the nitrogen excited state which allows pumping of the CO_2 molecules to occur downstream of the active discharge. It is not certain, however, to what extent mechanisms such as the current path deflection hypothesis suggested in reference 1 contribute to the gain-flow velocity relationship. For figure 5, as the flow velocity is increased from 60 to 110 meters per second, the downstream gain coefficient increases from 0.030 to 0.130 percent-centimeter^{-1}. At the same time the laser beam output power decreases from 4.9 to 3.9 kilowatts. These results lead to the conclusion that the optical-excitation configuration used was not efficiently extracting the stored optical energy particularly at high gas flow velocities. At first glance, it would seem apparent that the laser beam output could be optimized by flowing the gas at the low velocities or by moving the discharge volume upstream of the optics. Localized gas heating resulted in plasma instabilities at velocities lower than 90 meters per second for the conditions investigated, therefore we moved the discharge volume relative to the optics. The active discharge volume was shifted upstream by deactivating several of the downstream rows of pins. Referring to figure 3, it can be seen that by selectively deactivating rows of downstream pins one effectively places part of the "downstream" region of gain within the physical boundary of the single-pass, unstable resonator optics. A plot of the downstream small-signal

gain as a function of average input power density for several excited row configurations is shown in figure 6. For the 16 row configuration, it is evident that the gain downstream at point B is a strong function of discharge power density. One would expect that if the optics were efficiently extracting the available energy, the gain downstream would eventually reach a constant value as the input power density increases. This is observed for both the 13 and 11 row configurations. However, for the 16 row configuration the gain continues to increase with input power density. Therefore, it can be concluded that the 16 row configuration and the given unstable-resonator is not efficiently extracting optical power. By removing rows the distance between the observation point and the last excited row is increased. Thus the time available for deactivation of the excited medium becomes longer resulting in a lower downstream gain (refs. 1, 4, and 5) for the 11 and 13 row configurations.

The overall efficiencies of the two multipin-to-plane excitation configurations with single-pass, unstable resonator optics are presented in figure 7 as a function of specific discharge power. The efficiency of the laser is defined as the ratio of laser beam output power to discharge power. In general, the 11 row excitation configuration is substantially more efficient than the 16 row configuration. At high input power levels, the 11 row excitation scheme is 13 percent more efficient than that for 16 rows, and as much as 33 percent more efficient at lower input powers. Also plotted on figure 7 are the efficiency results for a folded optical path with 21 rows excited. This three-pass configuration with the total path length of 6.3 meters extends the optical extraction volume beyond the active discharge region. The three-pass optical geometry is defined in figure 8. The centerlines of the two mirrors are 16.5 centimeters apart, and 21 rows of pins are excited. A magnification of 1.45 was used with this optical configuration. The observation points for the gain measurements made previously

are shown for reference. Note that the downstream point B now lies within the optics. In general, a factor of two increase in laser output power is achieved for the folded path optics as compared to the single pass optics for the same discharge operating conditions. Thus, more of the downstream gain is efficiently extracted. Similar results have been reported elsewhere (ref. 6). From figure 7, it is evident that at high input powers, an increase in efficiency of 30 percent is realized over that for the 11 row, single-pass, unstable resonator configuration. At lower power levels, increases as high as 100 percent may be achieved. Gain measurements further downstream of the folded path shown extremely low gain coefficients of less than 0.01 percent-centimeter^{-1}, with almost no dependence on flow velocity.

CONCLUSIONS

The results presented herein indicate that improved laser efficiencies and output powers can be obtained for electric discharge, flow stabilized, CW gas lasers through efficient coupling of the excited medium to the resonator optics. Specifically the effects of gain swept downstream of the active discharge volume must be included in the resonator design if efficient extraction of laser energy is desired. The use of the small-signal gain measurement as a diagnostic tool to aid in achieving optimum extraction of laser power has been demonstrated. In particular, the significant residual gain measured downstream of the 16 row, single-pass resonator configuration led to the improved three-pass, 21 row resonator configuration. A factor of two increase in laser output power was achieved for the folded path optics as compared to the single-pass optics at the same discharge conditions.

REFERENCES

1. Wutzke, S. A.; et. al.: CW Pin Discharge Laser. Westinghouse Electric Corp., 1974. (Available from NTIS as AD-A014649.)

2. Lancashire, R. B.; et. al.: The NASA High Power Carbon Dioxide Laser: A Versatile Tool for Laser Applications. NASA TM X-73485, 1976.

3. Rigrod, W. W.: Gain Saturation and Output Power of Optical Masers. J. Appl. Phys., vol. 34, no. 9, Sep. 1963, pp. 2602-2609.

4. Targ, Russell and Tiffany, William B.: Gain and Saturation in Transverse Flowing CO_2-N_2-He Mixtures. Appl. Phys. Lett., vol. 15, no. 9, Nov. 1969, pp. 302-304.

5. McQuillan, A. K.; and Carswell, A I.: Spatially Resolved Gain Measurements in a Flowing CO_2 Amplifier. Appl. Phys. Lett., vol. 17, no. 4, Aug. 1970, pp. 158-160.

6. Seguin, H. J.; and Sedgwick, G.: Low Voltage Gas Transport TE CO_2 Laser. Appl. Opt., vol. 11, no. 4, Apr. 1972, pp. 745-748.

TABLE I. - SMALL-SIGNAL GAIN TEST CONDITIONS

FOR OBSERVATION POINT A

LASER GAS COMPOSITION (H_2:N_2:CO_2) 10: 7:1 AT 90 TORR

21 ROWS EXCITED

DISCHARGE GAP 5 CENTIMETERS

Elapsed time, min:sec	Gas flow velocity, m/sec	Mass flow rate, kg/sec	Discharge power, kW	Specific power, kJ/kg	Gain, %/cm
00:00	110	0.786	0.00	0.00	-----
02:94	103	.741	13.06	17.62	0.057
03.34	104	.75[illegible]	16.34	21.79	.074
05:02	105	.757	23.57	31.14	.127
06:13	104	.755	30.81	40.81	.189
07:07	102	.746	38.05	51.01	.243
08:25	104	.759	46.31	61.01	.309
09:52	101	.749	55.61	74.25	.374
10:57	101	.752	65.66	87.31	.435
12:20	99.2	.743	76.86	103.4	.496
14:00	104	.763	31.45	41.22	.183
15:42	111	.815	30.74	37.73	.164
17:05	121	.896	31.40	35.04	.147
18:18	132	.984	30.81	31.31	.130
19:14	147	1.11	30.32	27.36	.110
21:30	93.0	.679	31.64	46.60	.179
22:02	83.0	.605	32.26	53.32	.203
00:00	108.0	0.754	0.00	0.00	-----
07:48	106	.761	55.40	72.80	0.391
09:11	120	.867	55.72	64.27	.351
10:31	133	.967	55.56	57.46	.314
12:17	146	1.08	54.88	50.96	.284
14:01	138	1.01	55.80	55.19	.292
15:15	120	.870	56.56	65.01	.323
17:15	94.1	.676	55.91	82.71	.386
18:38	82.9	.596	56.89	95.45	.413
19:50	69.6	.500	56.04	112.1	-----
24:47	131	.964	59.32	61.54	.300
26:37	145	1.075	58.74	54.64	.274
00:00	108	0.767	0.00	0.00	-----
01:59	108	.800	76.32	95.40	0.521
03:44	128	.960	76.97	80.18	.435
05:35	136	1.03	77.36	75.18	.401
06:49	144	1.09	76.32	69.76	.372
09:04	133	1.01	77.24	76.70	.388
10:42	119	.896	77.64	86.65	.414
14.44	96.4	.718	78.93	109.9	.490

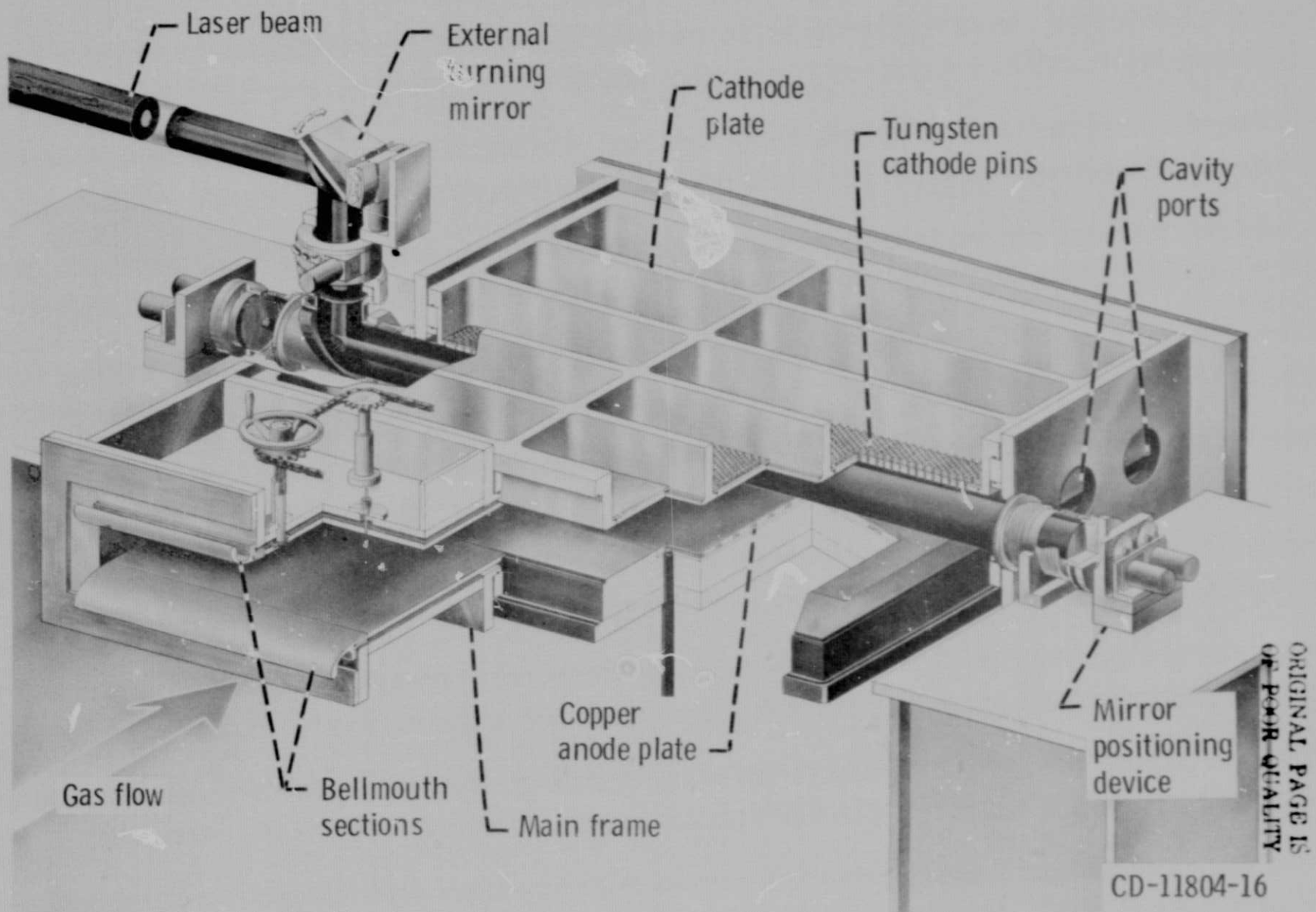

Figure 1. - Laser test cavity with pin-to-plane self-sustained discharge.

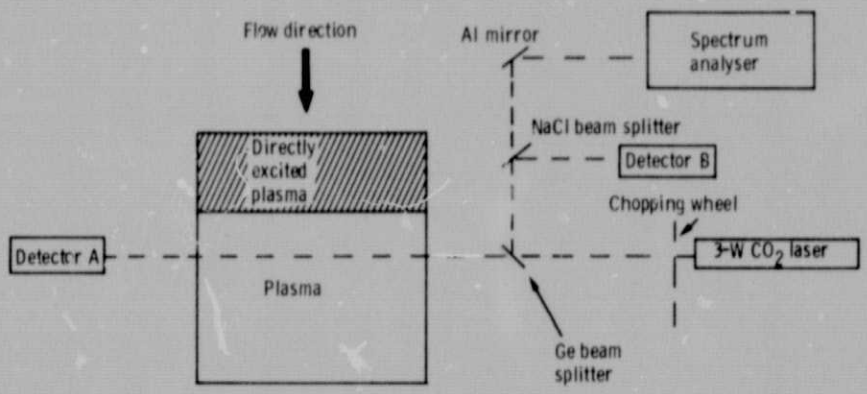

Figure 2. - Small signal gain test configuration.

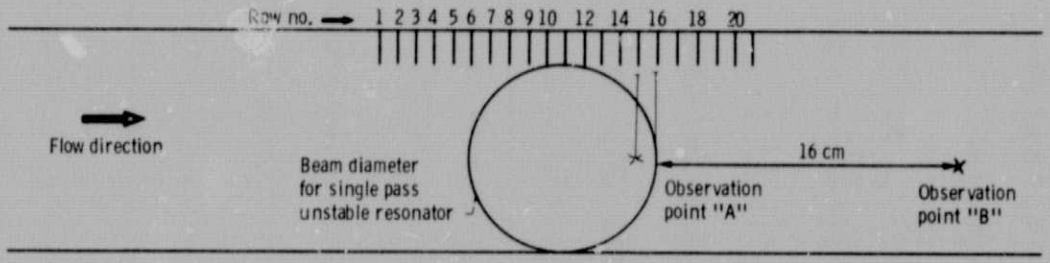

Figure 3. - Discharge geometry. 0.5372 cm spacing between rows. Measurement at point "A" w/o optics, 21 rows excited. Measurement at point "B" with optics, 16 rows excited.

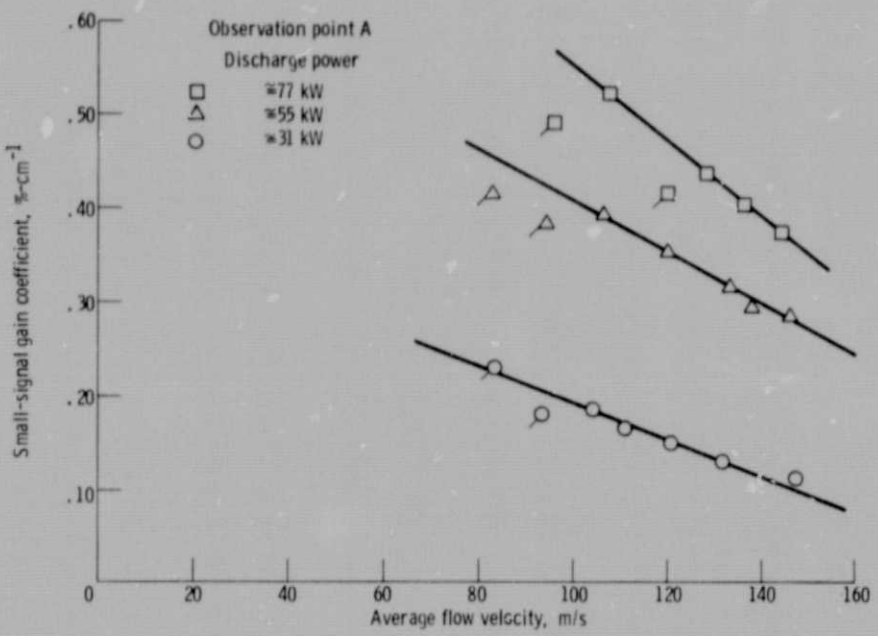

(a) Small-signal gain coefficient vs avg. flow velocity 10:7:1 mix at 90 torr total pressure. 5 cm discharge gap - 21 rows excited.

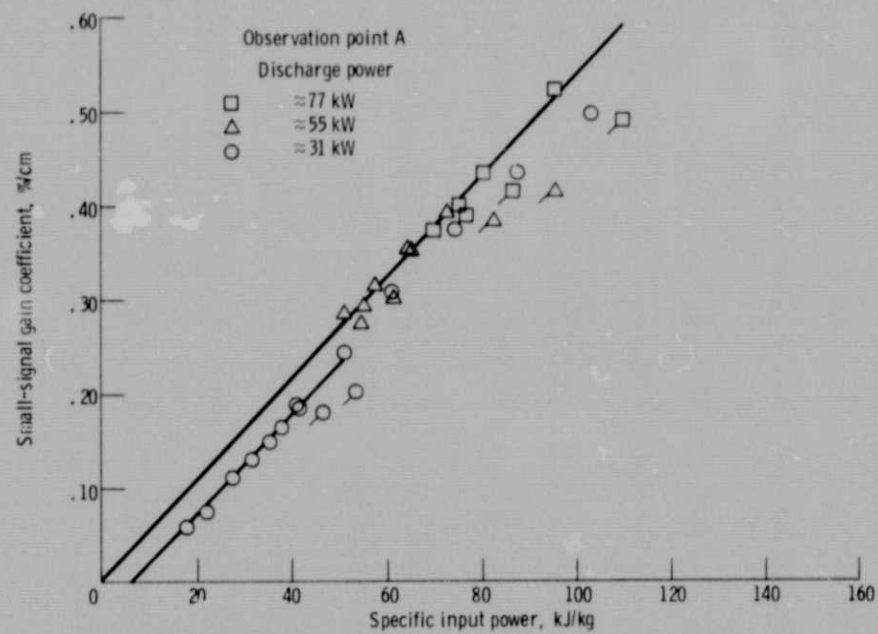

(b) Small-signal gain coefficient vs specific input power 10:7:1 mix at 90 torr total pressure. 5 cm discharge gap - 21 rows excited.

Figure 4.

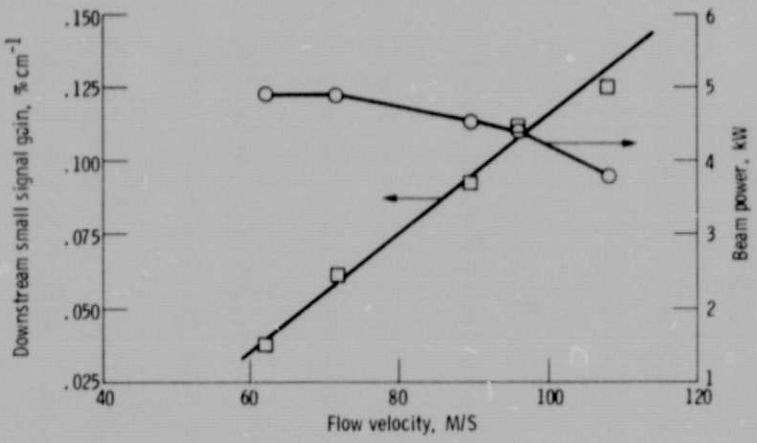

Figure 5. - Downstream gain and beam power vs flow velocity. 5 cm discharge gap. Unstable resonator configuration. 16 rows excited mix 10:7:1 at 90 torr. 53.4 kW discharge power.

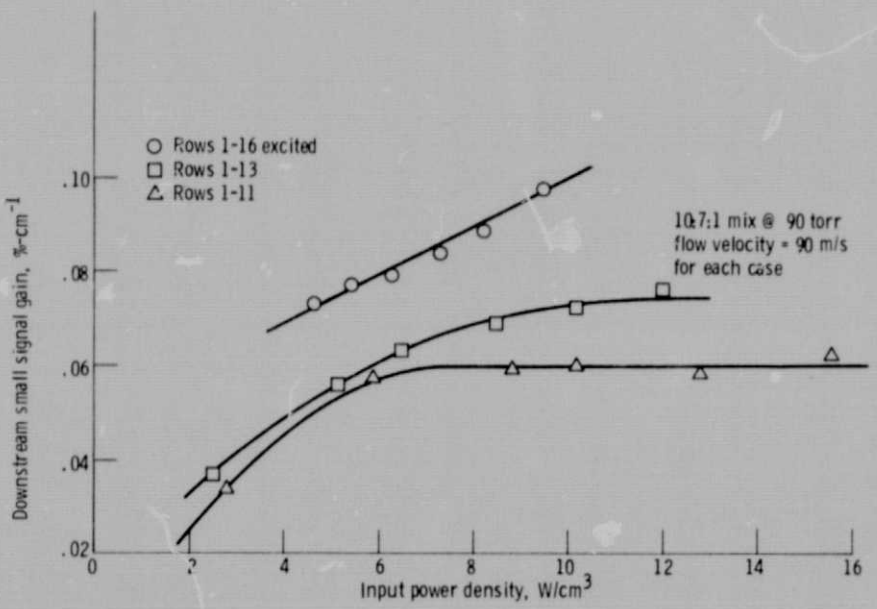

Figure 6. - Downstream small signal gain vs input power density. Single pass unstable resonator configuration. 5 cm discharge gap. Observation point "B".

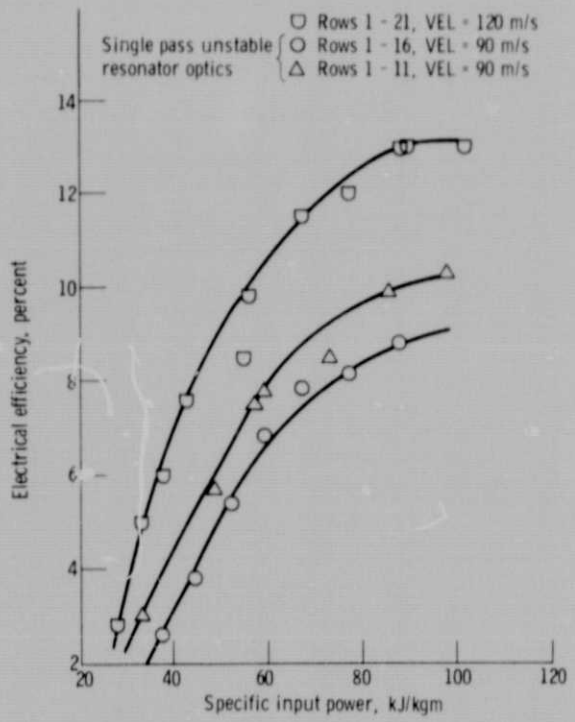

Figure 7. - Electrical efficiency vs specific discharge power. 10:7:1 mix at 90 torr. 5 cm discharge gap.

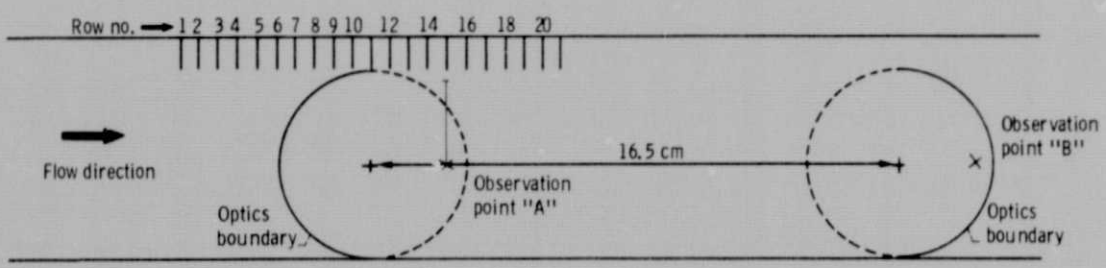

Figure 8. - Discharge/optics geometry for multipass configuration. 21 rows excited. 0.5372 cm spacing between rows. Extraction volume extends between mirrors.